LETTER • OPEN ACCESS

Estimating photosynthetic capacity from optimized Rubisco–chlorophyll relationships among vegetation types and under global change

To cite this article: Xuehe Lu *et al* 2022 *Environ. Res. Lett.* **17** 014028

View the article online for updates and enhancements.

ENVIRONMENTAL RESEARCH
LETTERS

LETTER

Estimating photosynthetic capacity from optimized Rubisco–chlorophyll relationships among vegetation types and under global change

Xuehe Lu[1,2,*] ⓘ, Holly Croft[3], Jing M Chen[4], Yiqi Luo[5] and Weimin Ju[2,6,*]

1   School of Geography Science and Geomatics Engineering, Suzhou University of Science and Technology, 99 Xuefu Road, Huqiu District, Suzhou, Jiangsu 215009, People's Republic of China
2   International Institute for Earth System Science, Nanjing University, Xianlin Avenue 163, Nanjing 210093, People's Republic of China
3   Department of Animal and Plant Sciences, University of Sheffield, Western Bank, Sheffield ST10 2TN, United Kingdom
4   Department of Geography, University of Toronto, Toronto, ON M5S 3G3, Canada
5   Center for Ecosystem Science and Society, Department of Biological Sciences, Northern Arizona University, Flagstaff, AZ 86001, United States of America
6   Jiangsu Center for Collaborative Innovation in Geographic Information Resource Development and Application, Nanjing, Jiangsu 210023, People's Republic of China
*   Authors to whom any correspondence should be addressed.

E-mail: luxh@usts.edu.cn and juweimin@nju.edu.cn

Abstract

The maximum rate of carboxylation (Vcmax), a key parameter indicating photosynthetic capacity, is commonly fixed as a constant by vegetation types and/or varies according to empirical scaling functions in Earth system models (ESMs). As such, the setting of Vcmax results in uncertainties of estimated carbon assimilation. It is known that the coupling between leaf chlorophyll and Rubisco (ribulose-1,5-biphosphate carboxylase-oxygenase) contents can be applied to estimate Vcmax. However, how this coupling is affected by environmental changes and varies among plant functional types (PFTs) has not been well investigated yet. The effect of varying coupling between chlorophyll and Rubisco contents on the estimation of Vcmax is still not clear. In this study, we compiled data from 76 previous studies to investigate the coupling between Chlorophyll (Chl) and Rubisco (Rub), in different PFTs and under different environmental conditions. We also assessed the ability of a Rub-based semi-mechanistic model to estimate Vcmax normalized to 25 °C (Vcmax$_{25}$) based on the Rub–Chl relationship. Our results revealed strong, linear Rub-Chl relationships for different PFTs ($R^2 = 0.73$, 0.67, 0.54 and 0.72 for forest, crop, grass and shrub, and C4 plants, respectively). The Rub–Chl slope of natural C3 PFTs was consistent and significantly different from those of crops and C4 plants. A meta-analysis indicated that reduced light intensity, elevated CO$_2$, and nitrogen addition strongly altered Rub/Chl. A semi-mechanistic model based on PFT-specific Rub–Chl relationships was able to estimate Vcmax$_{25}$ with high confidence. Our findings have important implications for improving global carbon cycle modeling by ESMs through the improved parameterization of Vcmax$_{25}$ using remotely sensed Chl content.

1. Introduction

Photosynthetic carbon assimilation is the principal driver of land carbon sink and represents the largest flux in the global carbon cycle (Schulze 2006, Keenan and Williams 2018, Luo *et al* 2019). Accurate estimation of photosynthetic carbon assimilation is a prerequisite for predicting land carbon cycle and carbon-climate feedbacks (Collins *et al* 2012). Within most Earth system models (ESMs), photosynthesis is modeled via the Farquhar–von Caemmerer–Berry (FvCB) kinetic enzyme scheme (Farquhar *et al* 1980). One of the key parameters used within the FvCB model to indicate photosynthetic capacity is

the maximum rate of carboxylation by the enzyme ribulose-1,5-biphosphate carboxylase-oxygenase (Rubisco), normalized to 25 °C ($Vcmax_{25}$). Therefore, accurate estimation of $Vcmax_{25}$ is essential to improve the performance of ESMs.

$Vcmax_{25}$ is determined by the amount and kinetics of the Rubisco (Rub) enzyme (Sage *et al* 2008, Bar-On and Milo 2019). And it is known that $Vcmax_{25}$ varies among and within PFTs and is affected by environmental conditions (Smith *et al* 2019), leaf ontogeny, and plant growth stages (Croft *et al* 2017). However, $Vcmax_{25}$ is commonly fixed as a constant by vegetation types and/or varies according to empirical scaling functions in ESMs (Rogers 2014, Luo *et al* 2019). Because of the difficulty in modeling $Vcmax_{25}$ values over a complete range of spatial and temporal scales, uncertainty remains in the parameterization of the photosynthetic capacity and in the incorporation of interannual variability and long-term trends into ESMs (Piao *et al* 2013, Anav *et al* 2015, Baldocchi *et al* 2016).

Existing literature has shown different underlying vegetational aspects, in terms of biochemical, structural, and environmental controls on Vcmax for estimating this photosynthetic capacity parameter. The relationship between $Vcmax_{25}$ and leaf nitrogen content (Kattge *et al* 2009) is well established, as it is well recognized that leaf nitrogen content is closely related to leaf photosynthetic capacity (Sage *et al* 1987), although the photosynthetic enzyme Rub accounts for only approximately 10%–30% of the total leaf nitrogen content in various plant species (Evans 1989). This relationship breaks down when nitrogen in non-photosynthetic components (e.g. cell wall) varies independently, either by species or leaf age (Wilson *et al* 2000, Croft *et al* 2017). Walker *et al* (2014) also indicated that changes in leaf phosphorus content substantially affected the relationship between $Vcmax_{25}$ and leaf nitrogen. Based on the first principle in ecophysiology that assumes leaves minimize the summed unit costs of transpiration and carboxylation, optimal Vcmax was predicted from climate variables alone (Smith *et al* 2019). Remote sensing data has been used to derive $Vcmax_{25}$ at different scales. Zhang *et al* (2018) proved the strong correlation of $Vcmax_{25}$ with solar-induced chlorophyll fluorescence (SIF) in the Midwestern US corn-belt. Using a model-data fusion approach, $Vcmax_{25}$ was mapped globally with gross primary production (GPP) estimated from GOME-2 SIF data (He *et al* 2019). A study by Serbin *et al* (2012) directly related Vcmax to hyperspectral reflectance data using a partial least-squares regression method.

Remote sensing of leaf chlorophyll (Chl) content, a key light-harvesting trait (Thornber 1975), is another way to estimate Vcmax. Croft *et al* (2017) used leaf Chl content of four tree species measured in a temperate deciduous forest to estimate $Vcmax_{25}$ in different seasons. In this way, leaf Chl is a proxy

for photosynthetic nitrogen, in that plants optimize the allocation of leaf nitrogen between Chl and Rub to maximize photosynthetic rates under given resource availability (Hikosaka and Hirose 1997, Prentice *et al* 2014). The empirical relationship between leaf Chl content and $Vcmax_{25}$ may provide a new way to map $Vcmax_{25}$ on a large scale because leaf Chl content could be retrieved from satellite imagery at a relatively high level of accuracy (Xu *et al* 2019, Croft *et al* 2020). However, the investigations in crops and other natural ecosystems illustrated that the coefficients of this relationship vary with different vegetation types obviously (Wang *et al* 2020, Qian *et al* 2021). This poses a challenge for mapping $Vcmax_{25}$ on a large scale when adopting $Vcmax_{25}$-Chl relationship.

Various previous studies indicated the correlation between $Vcmax_{25}$ and $Jmax_{25}$ because they are related to two coupled pivotal processes in photosynthesis, light energy harvesting by Chl and CO_2 assimilation in the Calvin-Benson cycle by Rub, respectively (Medlyn *et al* 2002, Walker *et al* 2014). Therefore, underlying the process of photosynthesis, the correlation between Chl and Rub can be expected. Driven by leaf Chl content, $Vcmax_{25}$ can also be simulated using a Rub-based semi-mechanistic model (Houborg *et al* 2013). In this model, leaf Chl content is a proxy of leaf Rub content. Lu *et al* (2020) demonstrated the strong correlation between leaf Chl and Rub contents over the whole growing season of winter wheat. And the $Vcmax_{25}$ simulated better by Rub-Chl relationship than by $Vcmax_{25}$-Chl relationship. Because the absorption of light energy by Chl and the amount of CO_2 catalyzed by Rub are tightly coupled in photosynthetic physiology (Evans 1989, Carmo-Silva *et al* 2015), the high robustness of Rub-Chl relationship in the same vegetation type can be assumed (Lu *et al* 2020). If this assumption is verified, the emerging mechanism of the coupling between leaf Chl and Rub contents will offer the potential to map $Vcmax_{25}$ at large scales.

The coupling between leaf Chl and Rub contents may be significantly affected by environmental conditions. Inside a forest canopy, for example, shade-acclimated leaves have higher Chl content to increase the utilization of diffuse light (Evans 1989, Posada *et al* 2009). Under elevated CO_2 conditions, the acclimation of photosynthetic processes results in a decrease in leaf Rub (Makino and Tadahiko 1999). Nitrogen addition in soils has been shown to increase both leaf Chl and Rub contents because more nitrogen is allocated to photosynthetic nitrogen pools, rather than structural components (e.g. leaf cell wall) (Bondada and Syvertsen 2003, Maekawa and Kokubun 2005).

Leaf Chl and Rub are therefore closely linked but differently affected by environmental factors. Quantification of their relationship under various environmental conditions is necessary to estimate Vcmax based on Rub kinetics using remotely sensed leaf Chl

content over large areas and under climate change. However, it is unclear whether Rub content can be a reliable intermediate variable to link Vcmax to Chl among PFTs. The possible impacts of the rising atmospheric CO_2 concentration, changing nitrogen deposition, and varying light conditions on the Rub-Chl relationship are also potentially important topics that have not been explored so far. Thus, this study was designed to (1) investigate the robustness of the relationship between leaf Chl and Rub contents in different PFTs; (2) analyze the impact of elevated atmospheric CO_2 concentrations, nitrogen deposition, and variations in light conditions on the Rub–Chl relationship via a meta-analysis; and (3) to assess the ability of a Rub-based semi-mechanistic model to estimate Vcmax$_{25}$ based on the Rub–Chl relationship. To address these issues, we primarily used observational data on leaf Chl, Rub, and Vcmax$_{25}$ from published literature.

2. Materials and methods

2.1. Data collection
Chlorophyll and Rub data were collected from previous studies (1990–2018) via a Web of Science search. A total of 1,043 results were found by searching 'chlorophyll Rubisco content.' A screening procedure was implemented to select studies that: (1) included synchronized observations of leaf Chl and Rub contents; (2) used area or mass units; and (3) had measurements of sunlit leaves, without treatments of CO_2, nitrogen, and light. In addition to this screening, studies with more than five observations in one growing season were treated specifically to explore the Rub–Chl relationship over time. For the meta-analysis, the studies were included if they reported (1) both Rub and Chl contents in the control and treatments (light, CO_2, or nitrogen) and (2) the means, standard deviations, and sample sizes for the control and each treatment.

After the screening procedure, 76 studies met the criteria (appendix A and table S1 (available online at stacks.iop.org/ERL/17/014028/mmedia)), and their spatial distributions are shown in figure 1.

To test the Rub–Chl relationship of different vegetation types at different locations, multiple measurements of Chl and Rub contents in a year for one species were averaged. In total, 132 observations were collected, of which 108 observations were reported in area units and 24 in mass units. To explore the Rub–Chl relationship that is applicable across the growing season, seven long-term observations reported in seven studies were collected (table S1). The numbers of observation data suitable for the meta-analysis of the impacts of light, CO_2, and nitrogen on the Rub–Chl relationship were 15, 21, and 31, respectively. Simultaneous measurements of Chl and Rub contents were directly collected from published tables or extracted from figures using the GetData

Graph Digitizer 2.24 (http://getdata-graph-digitizer.com).

2.2. Dummy variable regression analysis
A linear model was used to test the Rub–Chl relationship of different vegetation types at different locations and over time. Between species, the differences in the regression coefficients were tested through a dummy variable regression analysis, which is a widely used method to determine whether the coefficients of different regression lines are significantly different (Li *et al* 2010). First, the dummy variable was set to only 0 or 1 to identify the subsets of observations. Then, a multiple linear regression model was built with Rub content as the dependent variable and three independent variables (Chl content, dummy variable, and the product of the dummy variable and Chl content). Finally, multiple linear regression analysis was conducted using the R language to test the differences in the slope and intercept between the subsets of observations following the methods of Gujarati (1970).

2.3. Meta-analysis
Meta-analysis was first conducted to evaluate the effects of environmental changes on leaf Rub and Chl contents. Then, the changes in the ratio of Rub to Chl (Rub/Chl) were calculated using independent meta-analysis results of Rub and Chl contents to show the impacts of the environment on the relationship between Chl and Rub contents.

Response ratios (RRs) were calculated to evaluate the responses of Rub and Chl contents to light intensity, CO_2 enrichment and nitrogen addition. The RR of an individual experiment is defined in equation (1), which takes the logarithmic form to reduce bias and ensure a normal sampling distribution (Hedges *et al* 1999):

$$\ln RR = \ln \left(\frac{X_e}{X_c} \right) = \ln(X_e) - \ln(X_c), \quad (1)$$

where X_e and X_c are the average Chl and Rub contents of the experimental and control groups, respectively.

The corresponding variance for each $\ln RR$ was calculated as:

$$v = \frac{S_e^2}{n_e X_e^2} + \frac{S_c^2}{n_c X_c^2} \quad (2)$$

where S_e and S_c are the standard deviations of the experimental group and control group, respectively, and n_e and n_c are the sample sizes of the experimental and control groups, respectively. The integrated response ratio ($\overline{RR}$) is the weighted average of all individual RRs ($\ln RR_i$):

$$\overline{RR} = \frac{\sum (\ln RR_i \times w_i)}{\sum (w_i)}, \quad (3)$$

where $\ln RR_i$ is the response ratio of treatment *i*; w_i is the weighted coefficient, which is calculated as the reciprocal of *v*, that is,

Figure 1. Global distribution of studies included in this research. The sizes of circles represent the number of observations, ranging from 1 to 6.
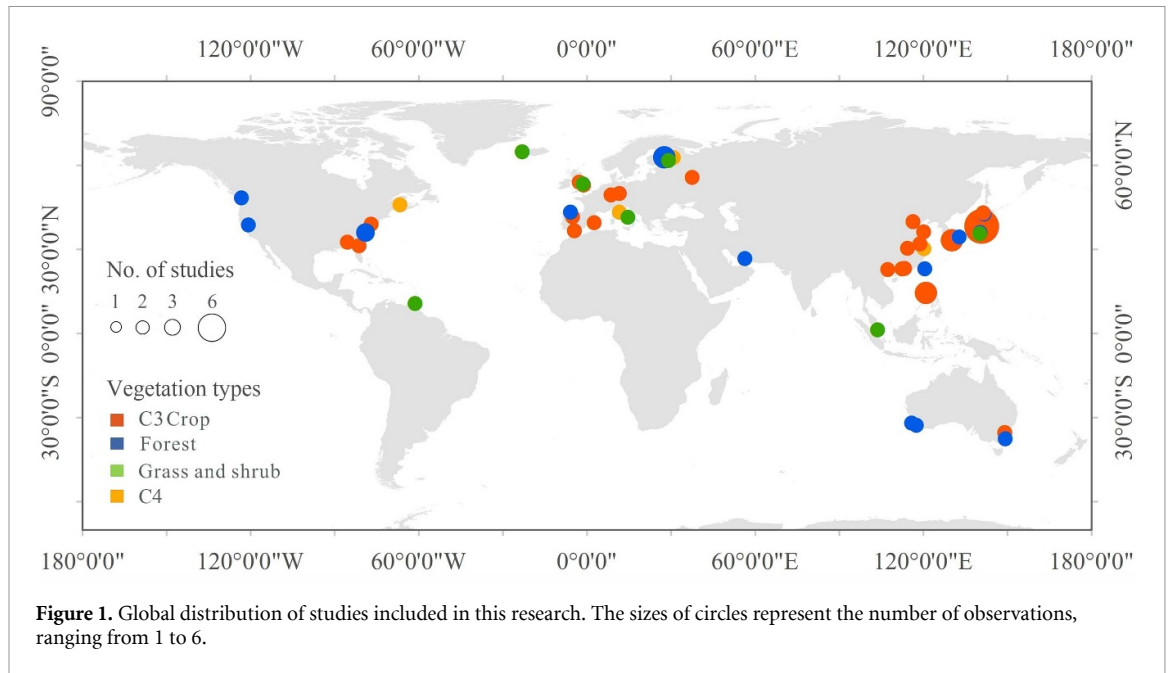
$$w_i = \frac{1}{v_i}. \qquad (4)$$

The integrated response ratio is converted to the percentage change D by:

$$D = \left(e^{\ln RR} - 1\right) \times 100\%. \qquad (5)$$

The 95% confidence interval (CI) value of $\overline{RR}$ is defined by:

$$CI = \overline{RR} \pm 1.96 SE$$
$$SE = \sqrt{\frac{1}{\sum w_i}}. \qquad (6)$$

2.4. Modeled Vcmax₂₅ by the Rub–Chl relationship
A Rub-based semi-mechanistic model is used to simulate Vcmax₂₅ (Friend 1995):

$$V_{\max}^{25} = K_{\mathrm{cat}}^{25} \cdot \frac{8}{550} \cdot R \cdot 10^3, \qquad (7)$$

where $V_{\max}^{25}$ is the Vcmax₂₅ (μmol CO_2 m^{-2} s^{-1}); K_{cat}^{25} is the Rub turnover rate at 25 °C (mol CO_2 mol sites^{-1} s^{-1}); R is leaf Rub content (g m^{-2}); $\frac{8}{550}$ is the constant used for converting Rub (kg) to moles of catalytic sites on Rub molecules, assuming the molecular weight of Rub to be 550 KD and 1 Rub molecule to have eight catalytic sites (Farquhar *et al* 1980); the constant of 10^3 is the product of 10^{-3} and 10^6, which converts the units of R and Vcmax₂₅ to kg m^{-2} and μmol m^{-2} s^{-1}, respectively.

Leaf Rub and Chl contents were assumed to be linearly correlated (Lu *et al* 2020):

$$R = a \cdot C + b, \qquad (8)$$

where C is the leaf Chl content (μg m^{-2}).

The K_{cat}^{25} is calculated in accordance with Eichelmann *et al* (2009):

$$K_{\mathrm{cat}}^{25} = \frac{e}{1 + d \cdot R_{\mathrm{mol}} \cdot 8}$$
$$R_{\mathrm{mol}} = R/0.55, \qquad (9)$$

where R_{mol} is the leaf Rub content in μmol m^{-2} and 0.55 is the constant (g μmol^{-1}) converted from the molecular weight of Rub, that is, 550 000 g mol^{-1}; d and e are coefficients.
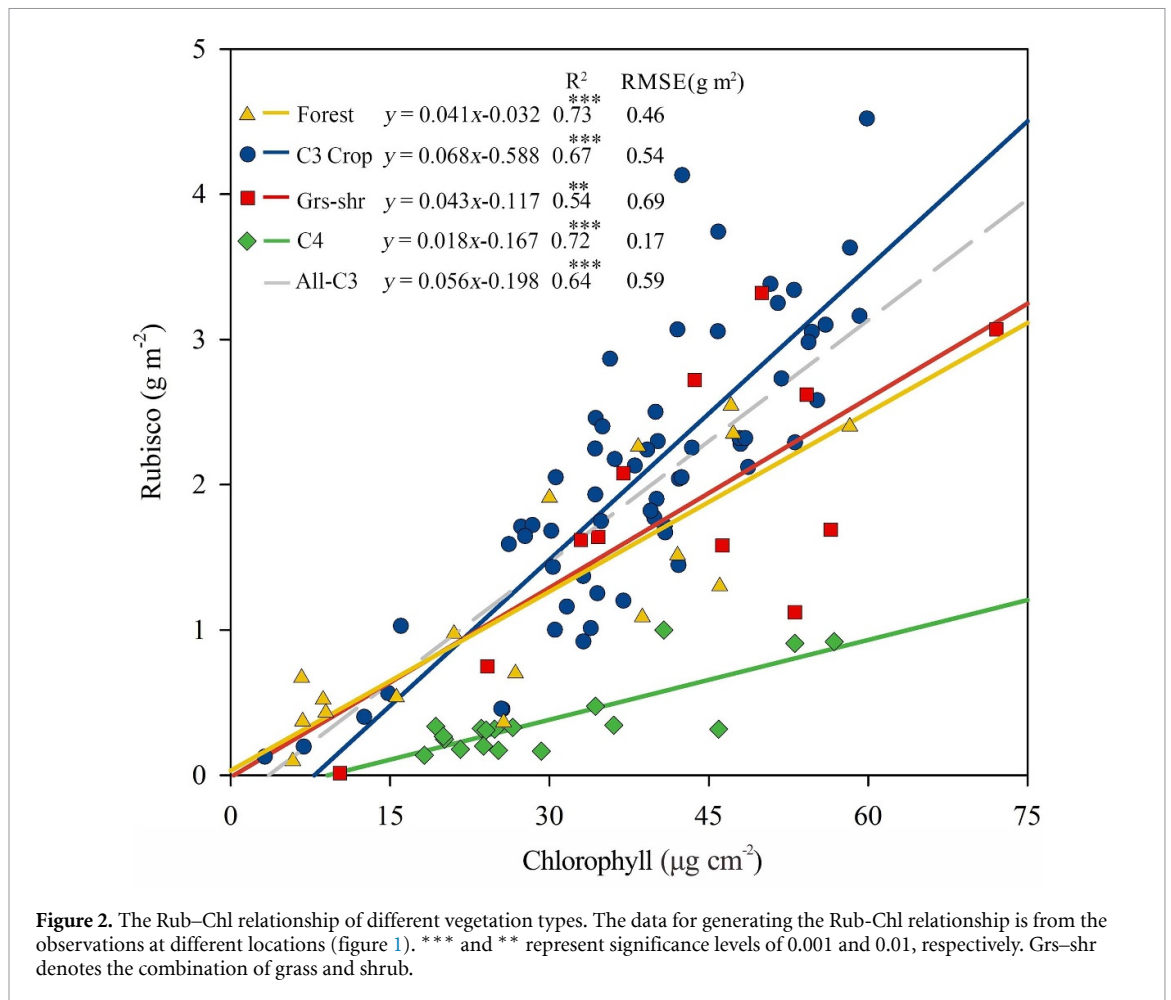
By combining equations (7)–(9), Vcmax₂₅ can be estimated as follows:

$$V_{\max}^{25} = \frac{800e(a.C + b)}{55 + 800d(a.C + b)}. \qquad (10)$$

In equation (8), coefficients a and b were fitted using our collected leaf Chl and Rub contents from previous studies (see section 2.1), while d and e in equation (10) were fitted to different PFTs using other collected Chl content and Vcmax₂₅ data from previous studies (Feng and Dietze 2013, Croft *et al* 2017, Migliavacca *et al* 2017, Wang *et al* 2020, Qian *et al* 2021) and our observations of a rice paddy and grassland in Jurong (31° 9 N, 119° 1 E) and Duolun (42° 2 N, 119° 17 E) ecological observatory stations in China, respectively (table S2). In these studies, Vcmax₂₅ and Chl were measured simultaneously. In order to determine Vcmax₂₅, the leaf carbon dioxide response curves were measured using the LI-6800 or LI-6400 portable infrared gas analyzers (LICOR, Lincoln, NE, USA). The details on the measurements of Vcmax₂₅ and Chl were described by Lu *et al* (2020).

For each PFT, a random selection of 50% of the paired Chl content and Vcmax₂₅ data was used to calibrate the parameters d and e in equation (10). And the remaining 50% of the paired Chl content and

Figure 2. The Rub–Chl relationship of different vegetation types. The data for generating the Rub-Chl relationship is from the observations at different locations (figure 1). *** and ** represent significance levels of 0.001 and 0.01, respectively. Grs–shr denotes the combination of grass and shrub.

$Vcmax_{25}$ data was used to validate the model independently.

3. Results

3.1. Relationships between leaf Chl and Rub contents in different vegetation types and overtime

The relationship between Chl and Rub contents was tested using 132 collected observations at different locations (figure 2). The collected data of C3 grass ($N = 5$) and shrub ($N = 7$) (grs–shr) were combined because their sample sizes were low. The C4 type included the observation of C4 grass ($N = 16$) and maize ($N = 2$). The leaf Chl content of all C3 plants was significantly correlated with leaf Rub content ($R^2 = 0.64$, $p < 0.001$, $N = 90$) in area units. A close relationship was also found in the mass units ($R^2 = 0.75$, $p < 0.001$, $N = 24$) (figure S1). As most of our collected observations (108 out of 132) and the leaf Chl content retrieved from remote sensing are expressed on an area basis, only those observations in area units were used for further analysis.
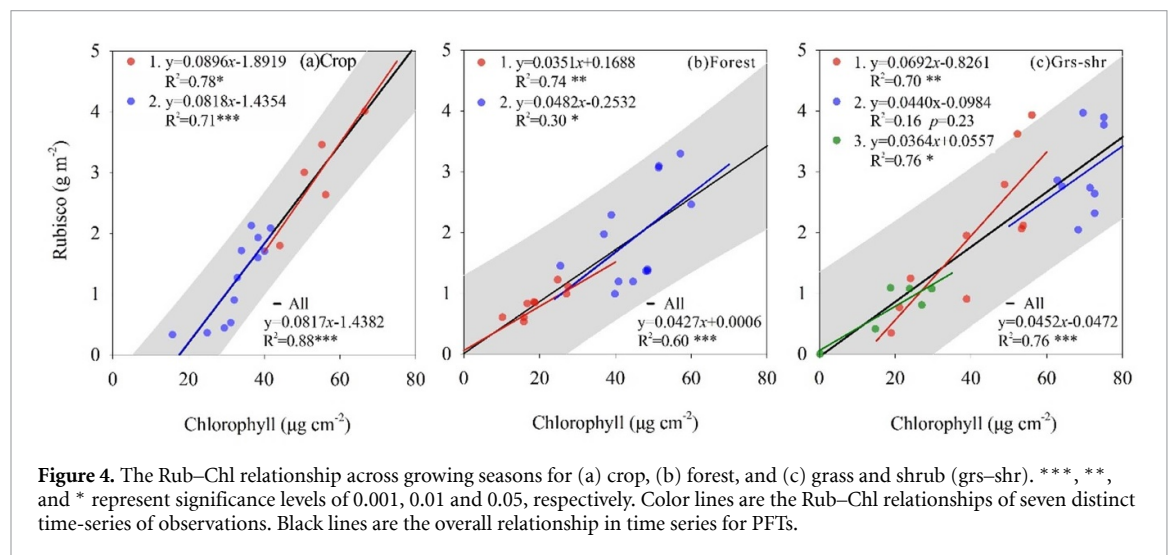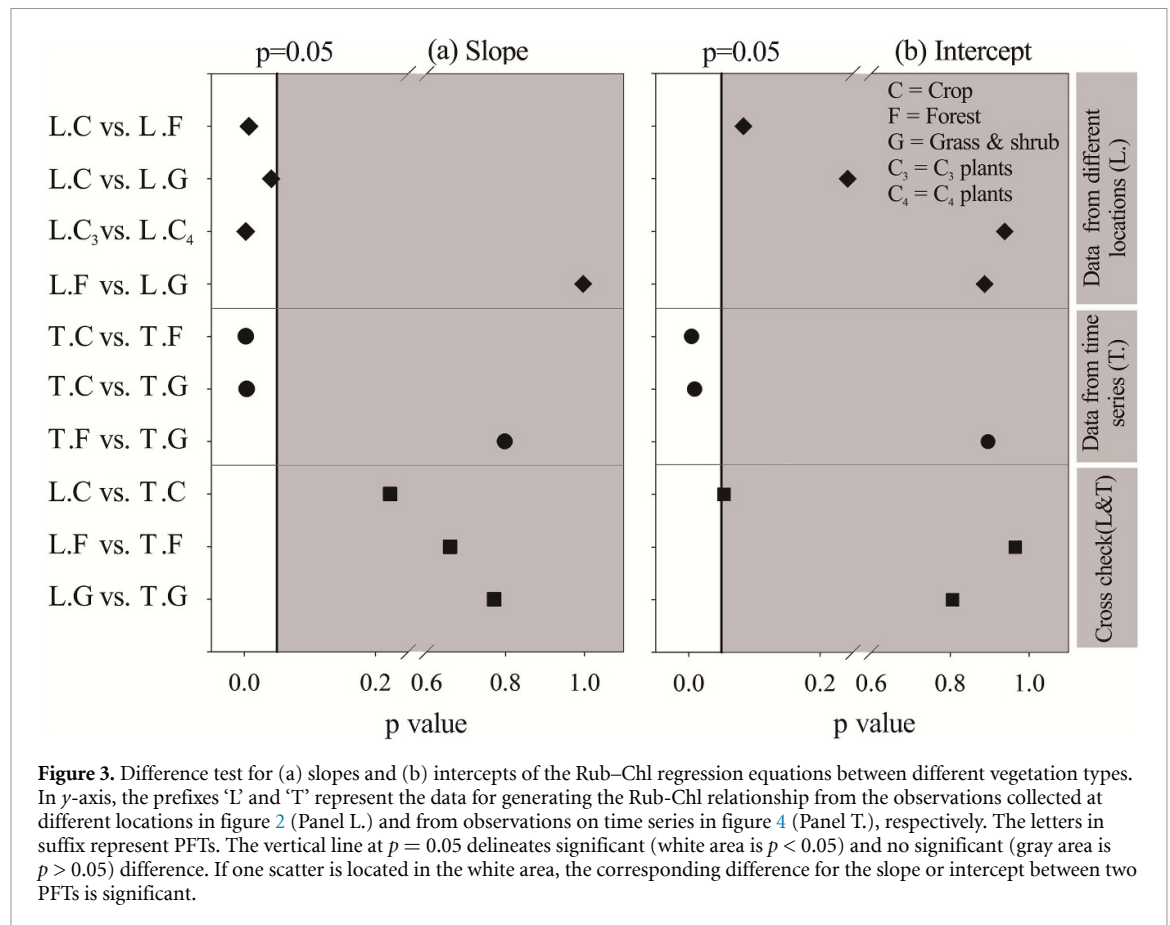
Strong linear relationships between Rub and Chl contents were found for individual (PFTs) (figure 2) according to the observations at different locations (figure 1). The R^2 values were 0.73 ($N = 17$, $p < 0.001$), 0.67 ($N = 61$, $p < 0.001$), 0.54 ($N = 12$,

$p < 0.01$), and 0.72 ($N = 18$, $p < 0.001$) for forest, crop, grs–shr, and C4 plants, respectively. And R^2 of grs-shr was lower than that of others. Owing to data limitation, grass and shrub were treated as the same PFT in the analysis. Their physiological and morphological differences could definitely affect the linearity of the Rub-Chl relationship for this combined PFT.

The dummy variable regression analysis indicated that the slope of the Rub–Chl relationship for crop (0.068) was significantly different from those of forest (0.041) and grs–shr (0.043) (panel L. in figure 3). The slopes of forest and grs–shr were not significantly different. The slope of C4 plants (0.018) was significantly lower than that of C3 plants (0.056) (panel L. in figure 3), due to the lower demand for Rub in C4 photosynthesis, where CO_2 carboxylation is under an anaerobic environment (Ehleringer *et al* 1991).

## 3.2. Seasonal changes of the relationships between leaf Chl and Rub contents

Leaf nitrogen allocation between the different photosynthetic (e.g. Chl and Rub) and non-photosynthetic pools (e.g. cell wall materials) changes with leaf ontological stages (Croft *et al* 2017), which might cause a seasonal change in the Rub–Chl relationship. Seven distinct time series of concurrent observations

Figure 3. Difference test for (a) slopes and (b) intercepts of the Rub–Chl regression equations between different vegetation types. In *y*-axis, the prefixes 'L' and 'T' represent the data for generating the Rub-Chl relationship from the observations collected at different locations in figure 2 (Panel L.) and from observations on time series in figure 4 (Panel T.), respectively. The letters in suffix represent PFTs. The vertical line at $p = 0.05$ delineates significant (white area is $p < 0.05$) and no significant (gray area is $p > 0.05$) difference. If one scatter is located in the white area, the corresponding difference for the slope or intercept between two PFTs is significant.

Figure 4. The Rub–Chl relationship across growing seasons for (a) crop, (b) forest, and (c) grass and shrub (grs–shr). ***, **, and * represent significance levels of 0.001, 0.01 and 0.05, respectively. Color lines are the Rub–Chl relationships of seven distinct time-series of observations. Black lines are the overall relationship in time series for PFTs.

of Chl and Rub contents were used to investigate whether the Rub–Chl relationship changed with seasons (figure 4). In each time series, the number of paired observations ranged from 5 to 12. Details on these seven distinct time series of observations are listed in table S1.

The linear correlations of leaf Chl and Rub contents were significant ($p < 0.001$) over time for different C3 PFTs (black line in each panel of figure 4), indicating that a uniform Rub–Chl relationship was applicable across seasons. Comparing the slopes of

different vegetation types in figure 4, the dummy variable analysis indicates that the slopes of the two C3 vegetation types, forest, and grs–shr, were close (T. panel in figure 3, $p > 0.05$) in time series, but their slopes were significantly lower than that of crops (T. panel in figure 3, $p < 0.05$). Meanwhile, no significant differences were found in the cross-comparisons among the Rub–Chl relationships shown in figures 2 and figure 4 in terms of the slope for the same PFTs (panel cross check in figure 3, $p > 0.05$). Therefore, for the same PFTs, the Rub–Chl
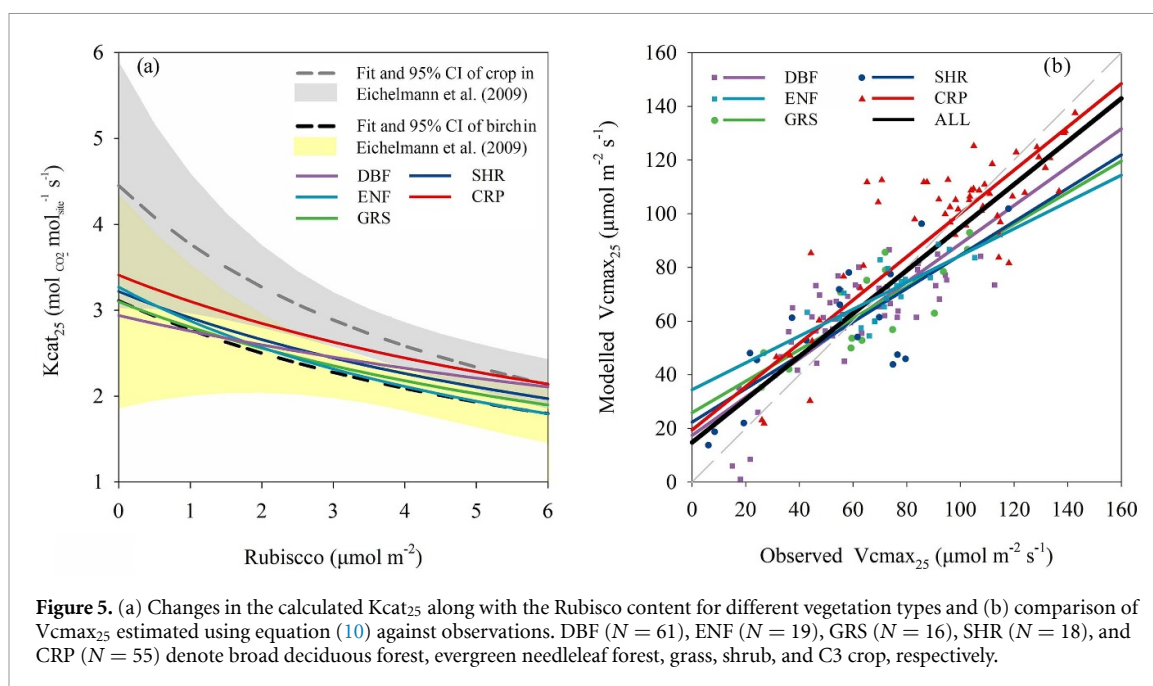
Figure 5. (a) Changes in the calculated $Kcat_{25}$ along with the Rubisco content for different vegetation types and (b) comparison of $Vcmax_{25}$ estimated using equation (10) against observations. DBF ($N = 61$), ENF ($N = 19$), GRS ($N = 16$), SHR ($N = 18$), and CRP ($N = 55$) denote broad deciduous forest, evergreen needleleaf forest, grass, shrub, and C3 crop, respectively.

relationships generated from the observations collected from varied locations (figure 1) and across growing seasons were comparatively consistent, which is conducive to $Vcmax_{25}$ estimation from leaf Chl content.

3.3. Modeled $Vcmax_{25}$ using the Rub–Chl relationship

Leaf Rub content and $Kcat_{25}$ are two key parameters for modeling $Vcmax_{25}$ using the Rub-based semi-mechanistic model shown in equation (7). The above analysis suggests that leaf Chl content is an effective proxy for leaf Rub content, while $Kcat_{25}$ can be estimated empirically using equation (9). The Rub–Chl relationship for each PFT shown in figure 2 was applied to the modeling leaf Rub content using leaf Chl content. Figure 5(b) shows a comparison of the modeled $Vcmax_{25}$ estimated on the basis of the Rub–Chl relationship against ground-based $Vcmax_{25}$ observations for different PFTs, including broad deciduous forest (DBF), evergreen needleleaf forest (ENF), grass (GRS), shrub (SHR), and crop (CRP).

Figure 5(a) shows the changes in $Kcat_{25}$ estimated by equation (9) along with the Rub content. The coefficients e and d of equation (9) fitted by paired measurements of $Vcmax_{25}$ and leaf Chl content collected from previous studies ranged from 2.94 (DBF) to 3.41 (CRP) and 0.008 (DBF) to 0.017 (ENF), respectively (table S3). Generally, our simulated $Kcat_{25}$ was in the range of 95% confidence interval (CI) fitted using the observed $Kcat_{25}$ and Rub content reported by Eichelmann *et al* (2009). As to the natural PFTs, including DBF, ENF, GRS, and SHR, the change in $Kcat_{25}$ along with the Rub content was close to that of birch reported by Eichelmann *et al* (2009). Our estimated $Kcat_{25}$ of crops was lower than that of

the corresponding value in the study of Eichelmann *et al* (2009), especially when leaf Rub content was in a low range (1–2 g m^{-2}). The change in $Kcat_{25}$ along with Rub content reported by Eichelmann *et al* (2009) was based on measurements on tobacco leaves. They pointed out that the tobacco species used in their experiment had low contents of Rub, with high turnover rates. As a consequence, the reported $Kcat_{25}$ was higher than our estimates.

Based on the strong relationship between leaf Chl and Rub contents, the estimated $Vcmax_{25}$ was generally consistent with observations ($R^2 = 0.75$ and RMSE $= 15.47 \ \mu\text{mol m}^{-2} \text{ s}^{-1}$ for all PFTs combined) (table 1). However, the slopes of all individual PFTs were lower than 1.0, indicating that low $Vcmax_{25}$ was overestimated, while high $Vcmax_{25}$ was underestimated systematically.

3.4. Effects of environmental factors on the Rub–Chl relationship

In order to identify the impacts of environmental conditions on the Rub–Chl relationship, a meta-analysis of different environmental drivers was performed (figure 6) across cropland and natural vegetation types (FGS, forest, grass and shrub). These drivers included light intensity, CO_2 enrichment and nitrogen fertilization as well as different treatments for each environmental variable.
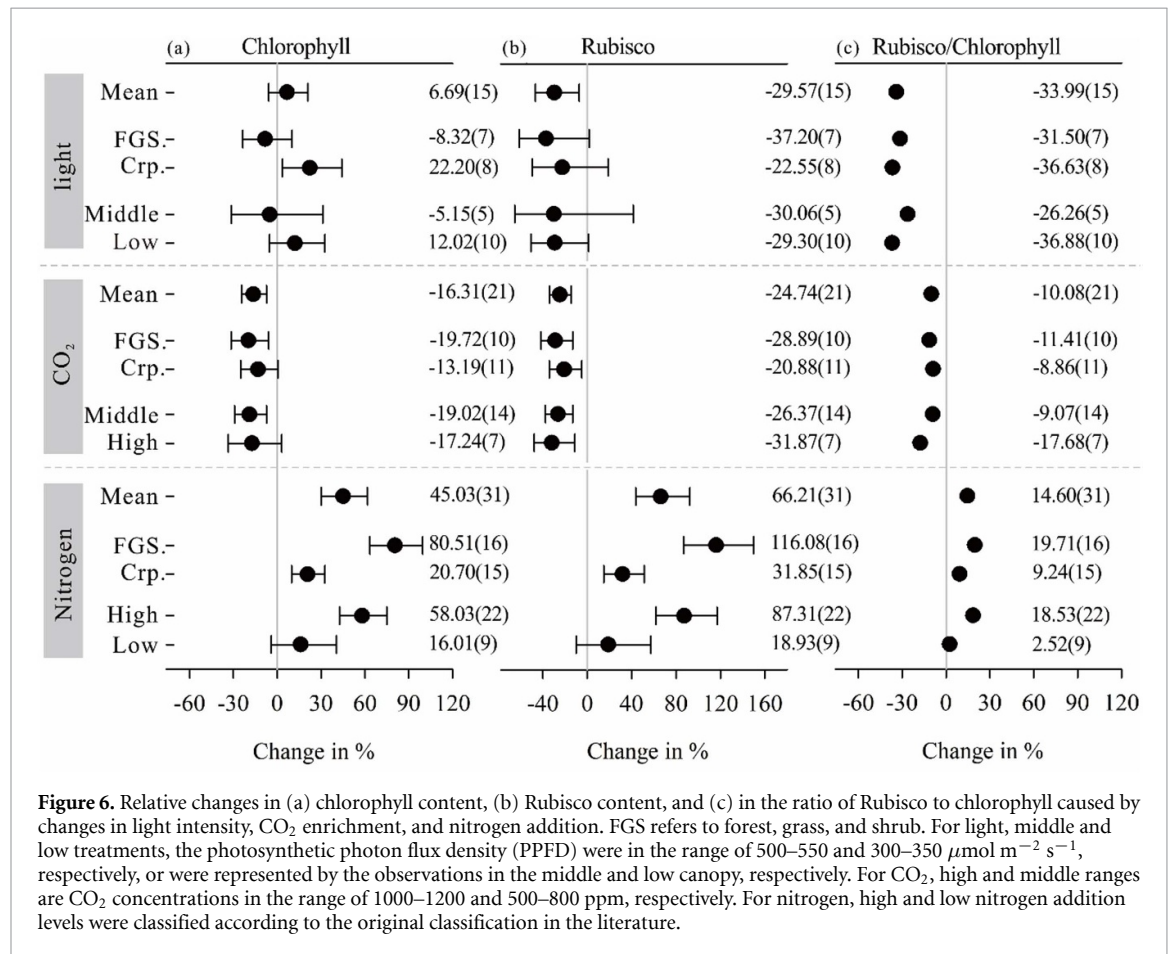
The metadata analysis indicates that a decrease in light intensity caused leaf Chl content to increase by 6.69% (figure 6(a)) and Rub content to decrease by 29.57% (figure 6(b)), on average. These changes led to a decrease in the Rub/Chl ratio by an average of 33.99% (figure 6(c)). The effect of light intensity on the Rub/Chl ratio has an important implication when the relationship established by observations on sunlit

Table 1. Comparison of modeled and observed Vcmax$_{25}$.

	Veg.	Full name of veg.	Slope	Inter.	R^2	RMSE
1	DBF	Broad deciduous forest	0.71	17.47	0.66	14.03
2	ENF	Evergreen needleleaf forest	0.52	34.47	0.52	10.26
3	GRS	Grass	0.59	25.90	0.65	14.21
4	SHR	Shrub	0.62	22.41	0.60	18.64
5	CRP	C3 Crop	0.81	19.50	0.74	17.53
6	ALL	All vegetation types	0.80	14.82	0.75	15.47

Note: Veg. and inter. are vegetation and intercept, respectively. R^2 is the determination coefficient. RMSE is the root mean square error
(μmol m^{-2} s^{-1}).

Figure 6. Relative changes in (a) chlorophyll content, (b) Rubisco content, and (c) in the ratio of Rubisco to chlorophyll caused by changes in light intensity, CO_2 enrichment, and nitrogen addition. FGS refers to forest, grass, and shrub. For light, middle and low treatments, the photosynthetic photon flux density (PPFD) were in the range of 500–550 and 300–350 μmol m^{-2} s^{-1}, respectively, or were represented by the observations in the middle and low canopy, respectively. For CO_2, high and middle ranges are CO_2 concentrations in the range of 1000–1200 and 500–800 ppm, respectively. For nitrogen, high and low nitrogen addition levels were classified according to the original classification in the literature.

leaves (figures 2 and 4) is used to estimate the Rub of shaded leaves within a canopy.

Figure 6(a) shows that a CO_2 enrichment of 500–1,200 ppm resulted in a significant decrease in Chl content by 16.31% on average. Rub content also exhibited a decrease under elevated CO_2 (figure 6(b)), which was stronger than the response of Chl content to elevated CO_2. Therefore, elevated CO_2 caused the Rub/Chl to decrease by 10.08% on average (figure 6(c)). The reduction of Rub/Chl caused by elevated CO_2 was stronger in natural ecosystems (FGS) (−11.41%) than in crop ecosystems (−8.86%).

On average, nitrogen addition induced Chl and Rub contents to increase by 45.03% (figure 6(a)) and 66.21% (figure 6(b)), respectively. In turn, the Rub/Chl increased by 14.06% (figure 6(c)). The addition of nitrogen to natural ecosystems resulted in larger increases in both Chl and Rub contents than its effects in crop ecosystems. High nitrogen addition increased Rub/Chl by 18.53%, which was higher than the increase in Rub/Chl (2.52%) under low nitrogen addition.

4. Discussion

4.1. The dynamic nature of the Rub–Chl relationship

The findings of this work confirm that leaf Chl and Rub contents were significantly correlated, as a result of their coordinated roles in plant photosynthesis (Evans 1989). The process of photosynthesis begins with light energy that is harvested by Chl molecules

to drive the synthesis of NADPH and ATP for storing chemical energy. This conversion from light energy to chemical energy takes place in the reaction centers of Photosystem II and Photosystem I in the chloroplast. The chemical energy is then used to drive the processes of CO_2 assimilation in the Calvin cycle. These processes are called carboxylation of CO_2 catalyzed by Rub. Previous studies have shown that Rub content is closely related to the quantities of reaction centers in Photosystem II (Krall and Edwards 1992, Ou *et al* 2003) and Photosystem I (Eichelmann *et al* 2004) in leaves, which are also determined by the leaf Chl content (Evans and Poorter 2001, Burns *et al* 2005). The correlation between leaf Chl and Rub content is due to the coupling between light harvesting and carboxylation processes to maximize photosynthesis (Carmo-Silva *et al* 2015).

In contrast to the complex changes in the relationship between leaf Chl and nitrogen contents during the growing season (Sage *et al* 1987, Evans 1989, Ghannoum *et al* 2005, Croft *et al* 2017), the correlation between leaf Chl and Rub contents was robust over time (figure 4). The nitrogen content in a leaf can be divided into structural nitrogen (such as cell walls) and photosynthetic nitrogen, including Chl and Rub. During the growing season, changes in the structural and photosynthetic nitrogen pools are dynamic (Hikosaka 2010, Houborg *et al* 2013). In this case, the total leaf nitrogen content is a poor indicator of photosynthetic capacity (Croft *et al* 2017). However, Chl and Rub are important pigments and enzymes, respectively, in photosynthetic physiology, and can be used as proxies to indicate nitrogen investment in photosynthesis (Scafaro *et al* 2017, Luo *et al* 2019). The Rub–Chl relationship avoids interference from the dynamics of nitrogen partition between structural and photosynthetic pools.
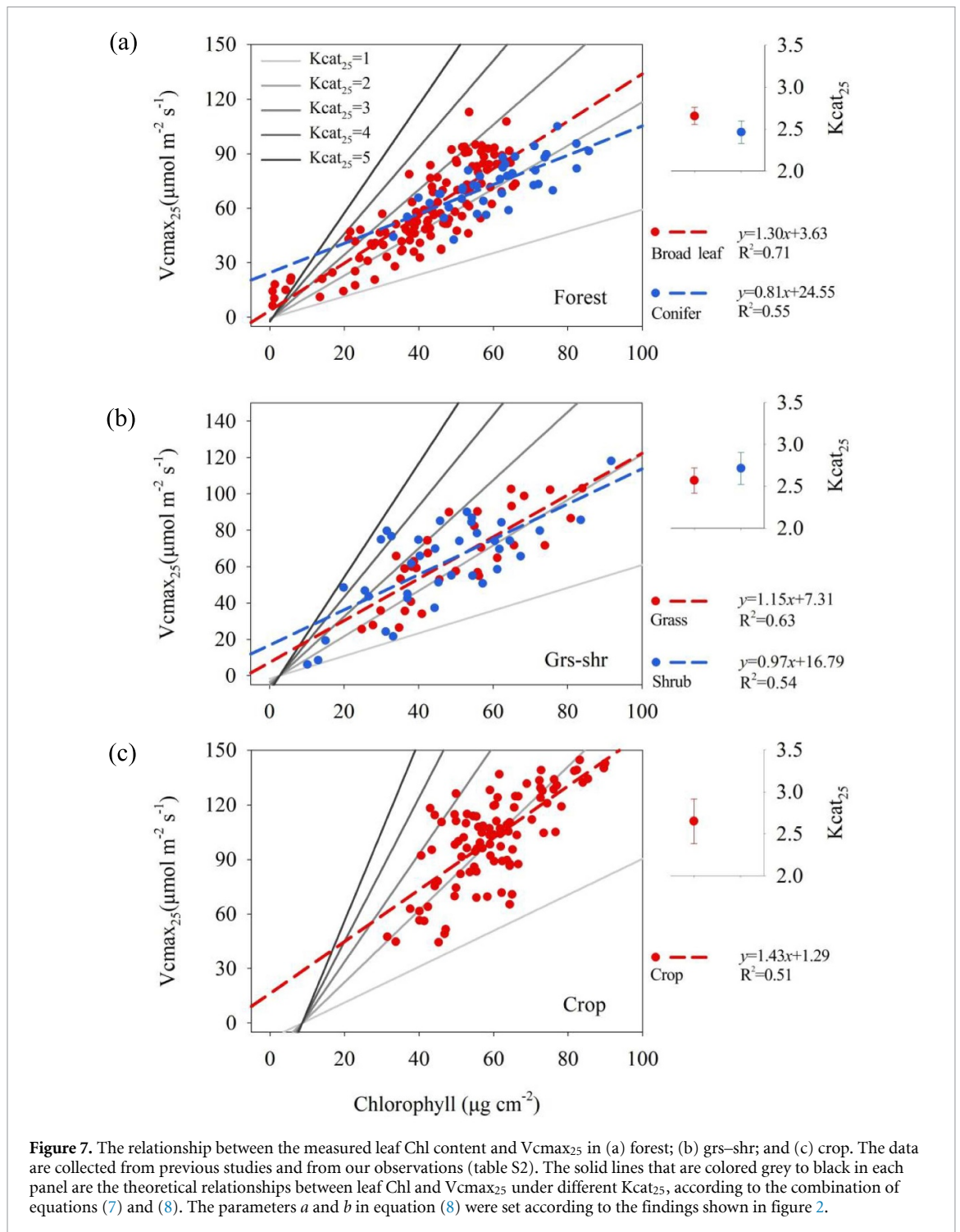
The linear relationship between leaf Chl content and $Vcmax_{25}$ was illustrated by a study within a deciduous forest in Canada (Croft *et al* 2017). According to equations (7) and (8), this relationship is linear for a given value of $Kcat_{25}$. However, if data with different values of $Kcat_{25}$ were lumped together, the relationship between leaf Chl content and $Vcmax_{25}$ would be nonlinear. In reality, $Kcat_{25}$ varies to some extent, caused by abiotic factors such as water supply, nutrient supply, temperature, among others (Bar-On and Milo 2019). Thus, the relationship between Chl and $Vcmax_{25}$ exhibits some nonlinearities when data collected under different environmental conditions are analyzed. As shown in figure 7, the linearity of the relationship between Chl and $Vcmax_{25}$ decreases with the variation in $Kcat_{25}$ within a specific PFT. The standard deviation of $Kcat_{25}$ of broad-leaf forest is the smallest (SD = 0.10 mol_{CO2} mol_{sites}^{-1} s^{-1}), and its linear relationship between Chl and $Vcmax_{25}$ is the strongest. The SD of $Kcat_{25}$ of the crop is the largest (SD = 0.27 mol_{CO2} mol_{sites}^{-1} s^{-1}), and its linear relationship between Chl and $Vcmax_{25}$ is the weakest

among all PFTs. Therefore, $Kcat_{25}$ has an impact on the robustness of the relationship between Chl and $Vcmax_{25}$. We suggest that this is one of the reasons why varied $Vcmax_{25}$-Chl relationships were found among PFTs in previous observation studies (Croft *et al* 2017, Wang *et al* 2020, Qian *et al* 2021).

4.2. Changes in Rub/Chl and implications for the estimation of carbon budgets

According to our study, natural ecosystems, including forests, grasslands, and shrubs, had a relatively stable slope for the Rub–Chl relationship across locations and over time. However, the slope of the C3 crop was different from those of the natural ecosystems (figure 3). Crops normally grow in an environment with artificial management such as fertilization and irrigation, which could be responsible for the higher slope in the Rub–Chl relationship. This was substantiated in figures 2 and 4, which demonstrated that an increase in the Rub/Chl slope for crops might be induced by nitrogen addition. While our meta-analysis results show that the average increase in Rub/Chl under nitrogen addition was approximately 14.6%, the slope of the Rub–Chl relationship for crops was about 64.0% higher than those of forests and grs–shr (figure 2). Therefore, the higher slope of the Rub–Chl relationship could be partially due to the difference in nitrogen richness between croplands and natural ecosystems. A further explanation may be due to breeding for the genetic optimization of crops. According to the studies of Makino and Sage (2007) and Sudo *et al* (2014), the Rub/Chl of transgenic crop plants with sense Rub small subunit (rbcS) was 42.12% higher than that of the wild type on average. To increase crop production, the processes of photosynthesis are manipulated to increase CO_2 assimilation by genetic engineering (Simkin *et al* 2019) or by classic breeding (Katsura *et al* 2007, Fujimoto *et al* 2012, Huang *et al* 2016), which also affects Rub/Chl in crops.

The findings in this study support the light-nitrogen hypothesis, Rub/Chl decreasing with the increase in shading (Warren and Adams 2001). The underlying cause of this decrease is the effect of light on the economics of nitrogen distribution (Field 1983, Friend 2001, Wright *et al* 2006). More nitrogen is allocated to the light harvesting apparatus used to capture light, thereby reducing the nitrogen allocation to Rub (Evans 1989, Posada *et al* 2009). Our meta-analysis added further evidence that the light-nitrogen hypothesis and showed that reduced light intensity caused Rub/Chl to decrease by 34.0% on average. Currently, ecosystem models have considered the different contributions of sunlight and shade leaves to canopy carbon assimilation (He *et al* 2013). Our study provides a correction to the Rub/Chl ratio via the light gradient, which will help improve the estimation of the photosynthetic rates of shade leaves in ESMs.

Figure 7. The relationship between the measured leaf Chl content and $Vcmax_{25}$ in (a) forest; (b) grs–shr; and (c) crop. The data are collected from previous studies and from our observations (table S2). The solid lines that are colored grey to black in each panel are the theoretical relationships between leaf Chl and $Vcmax_{25}$ under different $Kcat_{25}$, according to the combination of equations (7) and (8). The parameters *a* and *b* in equation (8) were set according to the findings shown in figure 2.

Many studies have shown that Rub reduces faster than any other photosynthetic component under CO_2 enrichment (Makino and Tadahiko 1999, Sudo *et al* 2014). Our meta-analysis also showed that the negative impact of elevated CO_2 on Rub was greater than that on Chl, which caused a decline in Rub/Chl. At the leaf scale, the decline in Rub, along with other photosynthetic components, is mainly due to the decrease in leaf nitrogen content caused by elevated CO_2 (Makino and Tadahiko 1999). Similar declines have been reported with observations in different vegetation types (Makino *et al* 1997, Ellsworth *et al*

2004, Bader *et al* 2013). The allocation of nitrogen to leaves is reduced by dilution resulting from increases in leaf area, plant mass, or by the allocation of nitrogen to leaf structure (Makino *et al* 1997, 1999, Norby *et al* 2010, Sardans *et al* 2017). Under the background of rising CO_2, the reduction in Rub caused by the decrease in leaf nitrogen content will affect the magnitude of CO_2 fertilization. Without consideration of this mechanism, the CO_2 fertilization effect may be currently overestimated by ESMs based on enzyme kinetics. The contribution of the increase in LAI caused by elevated CO_2 to global carbon

budgets should be further investigated (Winkler *et al* 2019).

Besides the environmental factors shown in figure 6, the impact of temperature on the Rub/Chl could not be neglected. In this study, we did not collect sufficient experimental data to investigate this impact. And since Rub and Chl are important for Vcmax and Jmax, respectively, this impact of temperature could be inferred from the previous studies focusing on the impact of temperature on Vcmax/Jmax. It is well-known that the ratio of Jmax to Vcmax declines with temperature (Medlyn *et al* 2002) because Jmax and Vcmax are differentially sensitive to temperature (Walker *et al* 2014). Such results of Vcmax/Jmax portend the unsynchronized changes of Chl and Rub under varied temperatures. Therefore, more temperature control experiments are needed to investigate how Rub/Chl change in the warming future.

4.3. Mapping Vcmax$_{25}$ through the Rub–Chl relationship

The maximum rate of carboxylation normalized to 25 °C exhibits large spatial and temporal variability (Groenendijk *et al* 2011, Smith *et al* 2019), and its accurate estimation can reduce the uncertainty of carbon budget simulation in ESMs (Kattge *et al* 2009, Rogers *et al* 2017, Luo *et al* 2019). In theory, plants coordinate resources to maximize the rate of photosynthesis (Prentice *et al* 2014). According to this 'coordination hypothesis' theory, Vcmax$_{25}$ can be calculated by optimizing the water cost in carboxylation (Smith *et al* 2019) or by optimizing the leaf utilization of nitrogen for carbon assimilation (Ali *et al* 2016). Our findings indicated the optimization between light harvest and carboxylation through the strong correlation between leaf Chl and Rub contents and therefore confirm the 'coordination hypothesis' theory. Combined with the remotely sensed leaf Chl content (Croft *et al* 2013, 2020, Xu *et al* 2019), the Rub–Chl relationship has a potential application in mapping Vcmax$_{25}$. The high robustness of the Rub–Chl relationship within vegetation types under ambient conditions is critical for mapping Vcmax$_{25}$ because current empirical models have large uncertainties in prescribed parameters for simulating carbon fluxes over large spatiotemporal scales (Rogers *et al* 2014). The close Rub–Chl relationship in natural ecosystems makes it possible to map the Rub content using a uniform set of parameters by remotely sensed Chl content.

Remotely sensed SIF (Solar-Induced Chlorophyll Fluorescence) is the most popular metric to improve the simulation of carbon assimilation. Its empirical relationship with Vcmax$_{25}$ was pointed out by the model study at eddy-covariance fluxes tower (Zhang *et al* 2018) and by *in-situ* observations (Li *et al* 2020). However, the sensitivity of SIF to Vcmax is likely low because Vcmax is involved in the dark reaction of

photosynthesis whereas SIF is emitted during the light reactions of photosynthesis (Frankenberg *et al* 2018). As a result, empirical estimation of Vcmax$_{25}$ through remotely sensed SIF still needs further research. And the fusion of remotely sensed SIF into terrestrial biosphere models has been illustrated as an effective way to optimize Vcmax$_{25}$ at a global scale (He *et al* 2019, Wang *et al* 2021).

The Kcat$_{25}$ is a key parameter affecting Vcmax$_{25}$ estimated according to the Rub–Chl relationship (equations (7) and (8)). Eichelmann *et al* (2009) proposed an empirical method to estimate Kcat$_{25}$. The applicability of this method was substantiated in this study. The averages of our estimated Kcat$_{25}$ ranged from 2.46 mol_{CO2} mol_{sites}^{-1} s^{-1} (conifer) to 2.71 mol_{CO2} mol_{sites}^{-1} s^{-1} (shrub) (table S4), in the range of mean C3 plants Kcat$_{25}$ (2.99 $\pm$ 0.58 mol_{CO2} mol_{sites}^{-1} s^{-1}) reported by Flamholz *et al* (2019). Our estimated Kcat$_{25}$ showed some variations within the same PFT. The SD values of the estimated Kcat$_{25}$ ranged from 0.10 mol_{CO2} mol_{sites}^{-1} s^{-1} (broad leaf forest) to 0.27 mol_{CO2} mol_{sites}^{-1} s^{-1} (C3 crop) (table S4). The small SD values of individual PFTs imply that the mean values of our estimated Kcat$_{25}$ are directly applicable for the regional and global mapping of Vcmax$_{25}$. Of course, this simplification would definitely induce uncertainties in the estimated Vcmax$_{25}$. The Kcat$_{25}$ is tightly linked to Rub content (figure 5), which might be empirically estimated from the Chl content (figure 2). This provides another option to determine Kcat$_{25}$ for mapping Vcmax$_{25}$. It is worthy of further investigation to determine Kcat$_{25}$ for better mapping Vcmax$_{25}$ from remotely sensed Chl content using the semi-empirical mechanistic model.

The biases of modeling Vcmax$_{25}$ by coupling the Rub–Chl relationship into the Rub-based semi-mechanistic model in our study (figure 5(b)) indicate the uncertainties of the parameters and model structure. On the one hand, the empirical estimation of parameter Kcat$_{25}$ brings uncertainties into modeling Vcmax$_{25}$. On the other hand, insufficient Rub and Chl data collected from published literature at low or high values have reduced the reliability of the Rub–Chl relationship and have hampered the prediction of Vcmax$_{25}$. Further, the collected data from previous experimental studies indicated that global change factors such as elevated CO_2 and atmospheric nitrogen deposition induced changes in the Rub–Chl relationship. Methodical equations that can describe these effects are still unavailable. Further investigation is required to include these effects in the Rub-based semi-mechanistic model for better mapping Vcmax$_{25}$.

5. Conclusions

In this study, the relationships between leaf Chl and Rub content, in different PFTs and under different

environmental conditions were investigated by compiled data from 76 previous studies. The significant linear Rub–Chl relationships differed among natural C3 vegetation types, C3 crops, and C4 plants according to 108 observations at different locations. And seven distinct time series of concurrent observations of leaf Chl and Rub contents showed that the Rub-Chl relationships across locations and time were similar for the same PFTs. According to dummy variable regression analysis, natural C3 PFTs demonstrated a consistent Rub-Chl slope, which was significantly different from those of crop and C4 plants. Based on PFT-specific Rub–Chl relationships, a semi-mechanistic model was able to estimate $Vcmax_{25}$ by leaf Chl content with high confidence. Thus, leaf Chl content is a good proxy of Rub for estimating $Vcmax_{25}$ using the semi-mechanistic model. A meta-analysis indicated the coupling between leaf Chl and Rub content was strongly affected by environmental changes, e.g. reduced light intensity, elevated CO_2, and nitrogen addition. Currently, these effects have not been incorporated into any models for estimating $Vcmax_{25}$. We suggest further investigation for including these effects in the Rub-based semi-mechanistic model for better mapping $Vcmax_{25}$ under future climate. Our findings have important implications for improving global carbon cycle modeling by ESMs through the better parameterization of $Vcmax_{25}$ using remotely sensed leaf Chl content.

Data availability statement

All data that support the findings of this study are included within the article (and any supplementary files).

Acknowledgments

ORCID iD

Xuehe Lu https://orcid.org/0000-0001-5919-0097

References

Ali A A *et al* 2016 A global scale mechanistic model of photosynthetic capacity (LUNA V1.0) *Geosci. Model Dev.* **9** 587–606

Anav A *et al* 2015 Spatiotemporal patterns of terrestrial gross primary production: a review *Rev. Geophys.* **53** 785–818

Bader M K F, Leuzinger S, Keel S G, Siegwolf R T, Hagedorn F, Schleppi P and Körner C 2013 Central European hardwood trees in a high-CO_2 future: synthesis of an 8-year forest canopy CO_2 enrichment project *J. Ecol.* **101** 1509–19

Baldocchi D, Ryu Y and Keenan T 2016 Terrestrial carbon cycle variability *F1000Research* **5** 2371

Bar-On Y M and Milo R 2019 The global mass and average rate of rubisco *Proc. Natl Acad. Sci.* **116** 4738–43

Bondada B R and Syvertsen J P 2003 Leaf chlorophyll, net gas exchange and chloroplast ultrastructure in citrus leaves of different nitrogen status *Tree Physiol.* **23** 553–9

Burns R A, MacDonald C D, McGinn P J and Campbell D A 2005 Inorganic carbon repletion disrupts photosynthetic acclimation to low temperature in the cyanobacterium Synechococcus elongatus *J. Phycol.* **41** 322–34

Carmo-Silva E, Scales J C, Madgwick P J and Parry M A J 2015 Optimizing Rubisco and its regulation for greater resource use efficiency *Plant Cell Environ.* **38** 1817–32

Collins M, Chandler R, Cox P, Huthnance J, Rougier J and Stephenson D 2012 Quantifying future climate change *Nat. Clim. Change* **2** 403–9

Croft H *et al* 2020 The global distribution of leaf chlorophyll content *Remote Sens. Environ.* **236** 111479

Croft H, Chen J M, Luo X, Bartlett P, Chen B and Staebler R M 2017 Leaf chlorophyll content as a proxy for leaf photosynthetic capacity *Glob. Change Biol.* **23** 3513–24

Croft H, Chen J M, Zhang Y and Simic A 2013 Modelling leaf chlorophyll content in broadleaf and needle leaf canopies from ground, CASI, Landsat TM 5 and MERIS reflectance data *Remote Sens. Environ.* **133** 128–40

Ehleringer J R, Sage R F, Flanagan L B and Pearcy R W 1991 Climate change and the evolution of C4 photosynthesis *Trends Ecol. Evol.* **6** 95–99

Eichelmann H, Oja V, Rasulov B, Padu E, Bichele I, Pettai H, Niinemets Ü and Laisk A 2004 Development of leaf photosynthetic parameters in Betula pendula Roth leaves: correlations with photosystem I density *Plant Biol.* **6** 307–18

Eichelmann H, Talts E, Oja V, Padu E and Laisk A 2009 Rubisco in planta kcat is regulated in balance with photosynthetic electron transport *J. Exp. Bot.* **60** 4077–88

Ellsworth D S, Reich P B, Naumburg E S, Koch G W, Kubiske M E and Smith S D 2004 Photosynthesis, carboxylation and leaf nitrogen responses of 16 species to elevated pCO2 across four free-air CO_2 enrichment experiments in forest, grassland and desert *Glob. Change Biol.* **10** 2121–38

Evans J R 1989 Photosynthesis and nitrogen relationships in leaves of C3 plants *Oecologia* **78** 9–19

Evans J R and Poorter H 2001 Photosynthetic acclimation of plants to growth irradiance: the relative importance of specific leaf area and nitrogen partitioning in maximizing carbon gain *Plant Cell Environ.* **24** 755–67

Farquhar G D, Von Caemmerer S and Berry J A 1980 A biochemical model of photosynthetic CO_2 assimilation in leaves of C3 species *Planta* **149** 78–90

Feng X and Dietze M 2013 Scale dependence in the effects of leaf ecophysiological traits on photosynthesis: Bayesian parameterization of photosynthesis models *New Phytol.* **200** 1132–44

Field C 1983 Allocating leaf nitrogen for the maximization of carbon gain: leaf age as a control on the allocation program *Oecologia* **56** 341–7

Flamholz A I, Prywes N, Moran U, Davidi D, Bar-On Y M, Oltrogge L M, Alves R, Savage D and Milo R 2019 Revisiting trade-offs between Rubisco kinetic parameters *Biochemistry* **58** 3365–76

Frankenberg C and Berry J 2018 Solar induced chlorophyll fluorescence: origins, relation to photosynthesis and retrieval *Comprehensive Remote Sensing* (Amsterdam: Elsevier) 143–62

Friend A D 2001 Modelling canopy CO_2 fluxes: are 'big-leaf' simplifications justified? *Glob. Ecol. Biogeogr.* **10** 603–19

Friend A 1995 PGEN: an integrated model of leaf photosynthesis, transpiration, and conductance *Ecol. Modell.* **77** 233–55

Fujimoto R, Taylor J M, Shirasawa S, Peacock W J and Dennis E S 2012 Heterosis of Arabidopsis hybrids between C24 and Col is associated with increased photosynthesis capacity *Proc. Natl Acad. Sci.* **109** 7109–14

Ghannoum O, Evans J R, Chow W S, Andrews T J, Conroy J P and Susanne V C 2005 Faster Rubisco is the key to superior

nitrogen-use efficiency in NADP-malicenzyme relative to NAD-malic enzyme C4 grasses *Plant Physiol.* **137** 638–50

Groenendijk M *et al* 2011 Assessing parameter variability in a photosynthesis model within and between plant functional types using global Fluxnet eddy covariance data *Agric. For. Meteorol.* **151** 22–38

Gujarati D 1970 Use of dummy variables in testing for equality between sets of coefficients in two linear regressions: a note *Am. Stat.* **24** 50–52

He L *et al* 2019 Diverse photosynthetic capacity of global ecosystems mapped by satellite chlorophyll fluorescence measurements *Remote Sens. Environ.* **232** 111344

He M *et al* 2013 Development of a two-leaf light use efficiency model for improving the calculation of terrestrial gross primary productivity *Agric. For. Meteorol.* **173** 28–39

Hedges L V, Gurevitch J and Curtis P S 1999 The meta-analysis of response ratios in experimental ecology *Ecology* **80** 1150–6

Hikosaka K 2010 Mechanisms underlying interspecific variation in photosynthetic capacity across wild plant species *Plant Biotechnol.* **27** 223–9

Hikosaka K and Hirose T 1997 Leaf angle as a strategy for light competition: optimal and evolutionarily stable light-extinction coefficient within a leaf canopy *Ecoscience* **4** 501–7

Houborg R, Cescatti A, Migliavacca M and Kustas W P 2013 Satellite retrievals of leaf chlorophyll and photosynthetic capacity for improved modeling of GPP *Agric. For. Meteorol.* **117** 10–23

Huang M, Shan S, Zhou X, Chen J, Cao F, Jiang L and Zou Y 2016 Leaf photosynthetic performance related to higher radiation use efficiency and grain yield in hybrid rice *Field Crops Res.* **193** 87–93

Katsura K, Maeda S, Horie T and Shiraiwa T 2007 Analysis of yield attributes and crop physiological traits of Liangyoupeijiu, a hybrid rice recently bred in China *Field Crops Res.* **103** 170–7

Kattge J, Knorr W, Raddatz T and Wirth C 2009 Quantifying photosynthetic capacity and its relationship to leaf nitrogen content for global-scale terrestrial biosphere models *Glob. Change Biol.* **15** 976–91

Keenan T F and Williams C A 2018 The terrestrial carbon sink *Annu. Rev. Environ. Resour.* **43** 219–43

Krall J P and Edwards G E 1992 Relationship between photosystem II activity and CO_2 fixation in leaves *Physiol. Plant.* **86** 180–7

Li J, Erickson J E, Peresta G and Drake B G 2010 Evapotranspiration and water use efficiency in a Chesapeake Bay wetland under carbon dioxide enrichment *Glob. Change Biol.* **16** 234–45

Li J, Zhang Y, Gu L, Li Z, Li J, Zhang Q, Zhang Z and Song L 2020 Seasonal variations in the relationship between sun-induced chlorophyll fluorescence and photosynthetic capacity from the leaf to canopy level in a rice crop *J. Exp. Bot.* **71** 7179–97

Lu X H, Ju W M, Li J, Croft H, Chen J M, Luo Y Q, Yu H and Hu H 2020 Maximum carboxylation rate estimation with chlorophyll content as a proxy of Rubisco content *J. Geophys. Res.: Biogeosci.* **125** e2020JG005748

Luo X, Croft H, Chen J M, He L and Keenan T F 2019 Improved estimates of global terrestrial photosynthesis using information on leaf chlorophyll content *Glob. Change Biol.* **25** 2499–514

Maekawa T and Kokubun M 2005 Correlation of leaf nitrogen, chlorophyll and rubisco contents with photosynthesis in a supernodulating soybean genotype Sakukei 4 *Plant Prod. Sci.* **8** 419–26

Makino A, Harada M, Sato T, Nakano H and Tadahiko M 1997 Growth and N allocation in rice plants under CO_2 enrichment *Plant Physiol.* **115** 199–203

Makino A and Mae T 1999 Photosynthesis and plant growth at elevated levels of CO_2 *Plant Cell Physiol.* **40** 999–1006

Makino A and Sage R F 2007 Temperature response of photosynthesis in transgenic rice transformed

with 'sense' or 'antisense' rbcS *Plant Cell Physiol.* **48** 1472–83

Medlyn B E *et al* 2002 Temperature response of parameters of a biochemically based model of photosynthesis. II. A review of experimental data *Plant Cell Environ.* **25** 1167–79

Migliavacca M *et al* 2017 Plant functional traits and canopy structure control the relationship between photosynthetic CO_2 uptake and far-red sun-induced fluorescence in a Mediterranean grassland under different nutrient availability *New Phytol.* **214** 1078–91

Norby R J, Warren J M, Iversen C M, Medlyn B E and McMurtrie R E 2010 CO_2 enhancement of forest productivity constrained by limited nitrogen availability *Proc. Natl Acad. Sci.* **107** 19368–73

Ou Z Y, Peng C L, Lin G Z and Yang C W 2003 Relationship between PSII excitation pressure and content of Rubisco large subunit or small subunit in flag leaf of super high-yielding hybrid rice *Acta Bot. Sin.* **45** 929–35

Piao S *et al* 2013 Evaluation of terrestrial carbon cycle models for their response to climate variability and to CO_2 trends *Glob. Change Biol.* **19** 2117–32

Posada J M, Lechowicz M J and Kitajima K 2009 Optimal photosynthetic use of light by tropical tree crowns achieved by adjustment of individual leaf angles and nitrogen content *Ann. Bot.* **103** 795–805

Prentice I C, Dong N, Gleason S M, Maire V and Wright I J 2014 Balancing the costs of carbon gain and water transport: testing a new theoretical framework for plant functional ecology *Ecol. Lett.* **17** 82–91

Qian X, Liu L, Croft H and Chen J 2021 Relationship between leaf maximum carboxylation rate and chlorophyll content preserved across 13 species *J. Geophys. Res.: Biogeosci.* **126** e2020JG006076

Rogers A 2014 The use and misuse of Vc,max in Earth System Models *Photosyn. Res.* **119** 15–29

Rogers A *et al* 2017 A roadmap for improving the representation of photosynthesis in Earth system models *New Phytol.* **213** 22–42

Sage R F, Pearcy R W and Seemann J R 1987 The nitrogen use efficiency of C3 and C4 plants : III. Leaf nitrogen effects on the activity of carboxylating enzymes in Chenopodiumalbum (L.) and Amaranthus retroflexus (L.) *Plant Physiol.* **85** 355–9

Sage R F, Way D A and Kubien D S 2008 Rubisco, Rubisco activase, and global climate change *J. Exp. Bot.* **59** 1581–95

Sardans J, Grau O, Chen H Y H, Janssens I A, Ciais P, Piao S and Peñuelas J 2017 Changes in nutrient concentrations of leaves and roots in response to global change factors *Glob. Change Biol.* **23** 3849–56

Scafaro A P, Xiang S, Long B M, Bahar N H A, Weerasinghe L K, Creek D, Evans J R, Reich P B and Atkin O K 2017 Strong thermal acclimation of photosynthesis in tropical and temperate wet-forest tree species: the importance of altered Rubisco content *Glob. Change Biol.* **23** 2783–800

Schulze E D 2006 Biological control of the terrestrial carbon sink *Biogeosciences* **3** 147–66

Serbin S P, Dillaway D N, Kruger E L and Townsend P A 2012 Leaf optical properties reflect variation in photosynthetic metabolism and its sensitivity to temperature *J. Exp. Bot.* **63** 489–502

Simkin A J, López-Calcagno P E and Raines C A 2019 Feeding the world: improving photosynthetic efficiency for sustainable crop production *J. Exp. Bot.* **70** 1119–40

Smith N G *et al* 2019 Global photosynthetic capacity is optimized to the environ-ment *Ecol. Lett.* **22** 506–17

Sudo E, Suzuki Y and Makino A 2014 Whole-plant growth and N utilization in transgenic rice plants with increased or decreased rubisco content under different CO_2 partial pressures *Plant Cell Physiol.* **55** 1905–11

Thornber J P 1975 Chlorophyll-proteins: light-harvesting and reaction center components of plants *Annu. Rev. Plant Physiol.* **26** 127–58

Walker A P, Beckerman A P, Gu L, Kattge J, Cernusak L A, Domingues T F, Scales J C, Wohlfahrt G, Wullschleger S D and Woodward F I 2014 The relationship of leaf photosynthetic traits—Vcmax and Jmax—to leaf nitrogen, leaf phosphorus, and specific leaf area: a meta-analysis and modeling study *Ecol. Evol.* **4** 3218–35

Wang J, Jiang F, Wang H, Qiu B, Wu M, He W, Ju W, Zhang Y, Chen J M and Zhou Y 2021 Constraining global terrestrial gross primary productivity in a global carbon assimilation system with OCO-2 chlorophyll fluorescence data *Agric. For. Meteorol.* **304–5** 108424

Wang S, Li Y, Ju W, Chen B, Chen J, Croft H, Mickler R A and Yang F 2020 Estimation of leaf photosynthetic capacity from leaf chlorophyll content and leaf age in a subtropical evergreen coniferous plantation *J. Geophys. Res.: Biogeosci.* **125** e2019JG005020

Warren C R and Adams M A 2001 Distribution of N, Rubisco and photosyn-thesis in Pinus pinaster and acclimation to light *Plant Cell Environ.* **24** 597–609

Wilson K B, Baldocchi D D and Hanson P J 2000 Spatial and seasonal variability of photosynthetic parameters and their relationship to leaf nitrogen in a deciduous forest *Tree Physiol.* **20** 565–78

Winkler A J, Myneni R B, Alexandrov G A and Brovkin V 2019 Earth sys tem models underestimate carbon fixation by plants in the high latitudes *Nat. Commun.* **10** 885

Wright I J, Leishman M R, Read C and Westoby M 2006 Gradients of light availability and leaf traits with leaf age and canopy position in 28 Australian shrubs and trees *Funct. Plant Biol.* **33** 407

Xu M, Liu R, Chen J M, Liu Y, Shang R, Ju W, Wu C and Huang W 2019 Retrieving leaf chlorophyll content using a matrix-based vegetation index combination approach *Remote Sens. Environ.* **224** 60–73

Zhang Y, Guanter L, Joiner J, Song L and Guan K 2018 Spatially-explicit monitoring of crop photosynthetic capacity through the use of space-based chlorophyll fluorescence data *Remote Sens. Environ.* **210** 362–74